AD-A085 219 ENVIRONMENTAL RESEARCH INST OF MICHIGAN ANN ARBOR F/G 20/6
COMPUTER GENERATED HOLOGRAPHIC OPTICS.(U)
MAY 80 J R FIENUP DAAG29-77-C-0017
UNCLASSIFIED ERIM-128600-12-F ARO-14582.2-EL NL

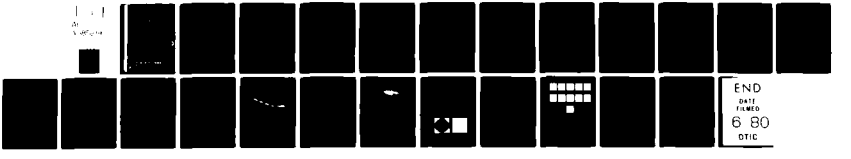

END
DATE FILMED
6 80
DTIC

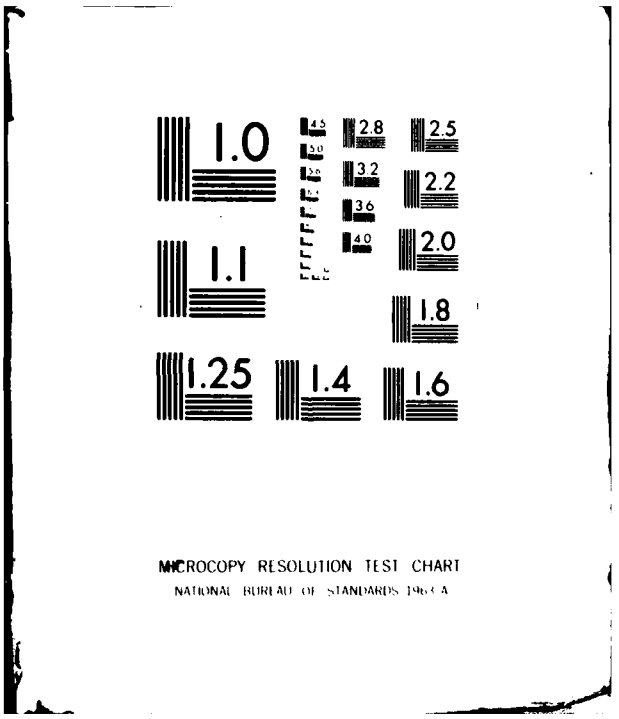
1.0
1.1
1.25
1.4
1.6
1.8
2.0
2.2
2.5
2.8
3.2
3.6
4.0
MICROCOPY RESOLUTION TEST CHART
NATIONAL BUREAU OF STANDARDS 1963 A

Final Report

COMPUTER GENERATED HOLOGRAPHIC OPTICS

J. R. FIENUP
Radar And Optics Division

MAY 1980

U.S. ARMY RESEARCH OFFICE
P.O. BOX 12211
RESEARCH TRIANGLE PARK, N.C. 27709

CONTRACT NO. DAAG29-77-C-0017

ENVIRONMENTAL
RESEARCH INSTITUTE OF MICHIGAN
BOX 8618 • ANN ARBOR • MICHIGAN 48107

DISCLAIMER NOTICE

THIS DOCUMENT IS BEST QUALITY PRACTICABLE. THE COPY FURNISHED TO DTIC CONTAINED A SIGNIFICANT NUMBER OF PAGES WHICH DO NOT REPRODUCE LEGIBLY.

UNCLASSIFIED
SECURITY CLASSIFICATION OF THIS PAGE (When Data Entered)

(18) ARO **REPORT DOCUMENTATION PAGE**

READ INSTRUCTIONS BEFORE COMPLETING FORM

(19) 1. REPORT NUMBER 14582.2-EL	2. GOVT ACCESSION NO. AD-A085219
3. RECIPIENT'S CATALOG NUMBER (9)	
(6) 4. TITLE (and Subtitle) COMPUTER GENERATED HOLOGRAPHIC OPTICS	5. TYPE OF REPORT & PERIOD COVERED Final Report 1 Apr 77 — 31 Mar 80
	6. PERFORMING ORG. REPORT NUMBER
(10) 7. AUTHOR(s) James R. Fienup	(15) 8. CONTRACT OR GRANT NUMBER(s) DAAG29-77-C-0017
9. PERFORMING ORGANIZATION NAME AND ADDRESS Environmental Research Institute of Michigan Box 8618 Ann Arbor, MI 48107	10. PROGRAM ELEMENT, PROJECT, TASK AREA & WORK UNIT NUMBERS
11. CONTROLLING OFFICE NAME AND ADDRESS U. S. Army Research Office Post Office Box 12211 Research Triangle Park, NC 27709	(11) 12. REPORT DATE May 80
	13. NUMBER OF PAGES ~~20~~ (12) 23
14. MONITORING AGENCY NAME & ADDRESS(if different from Controlling Office)	15. SECURITY CLASS. (of this report) Unclassified
	15a. DECLASSIFICATION/DOWNGRADING SCHEDULE

16. DISTRIBUTION STATEMENT (of this Report)

Approved for public release; distribution unlimited.

(14) ERIM-128600-12-F

17. DISTRIBUTION STATEMENT (of the abstract entered in Block 20, if different from Report)

NA

18. SUPPLEMENTARY NOTES

The view, opinions, and/or findings contained in this report are those of the author(s) and should not be construed as an official Department of the Army position, policy, or decision, unless so designated by other documentation.

19. KEY WORDS (Continue on reverse side if necessary and identify by block number)

computer programs
holograms
holographic optical elements
holographic lenses
ray-tracing

20. ABSTRACT (Continue on reverse side if necessary and identify by block number)

The goal of this research was to theoretically and experimentally investigate the use of computer-generated holograms in the design and fabrication of holographic optical elements (holographic lenses or diffraction optics). Conventional design of holographic lenses had previously been limited to spherical recording beams, and more recently to recording beams formed by conventional optical systems. The utilization of computer-generated holograms in the recording beams allows a completely arbitrary specification of the recording wavefronts in the hologram plane.

DD FORM 1 JAN 73 1473 EDITION OF 1 NOV 65 IS OBSOLETE

UNCLASSIFIED
SECURITY CLASSIFICATION OF THIS PAGE (When Data Entered)

40790 3

20. ABSTRACT CONTINUED

making possible a hologram lens of higher performance (lower aberrations) than previously possible. We refer to an interferometrically recorded hologram lens having a computer-generated hologram in a recording beam as a computer-originated holographic lens. We studied the basic limitations of computer-generated holograms, and integrated the analysis of computer-generated holograms and computer-originated holographic optical elements into ERIM's holographic optical analysis and design (HOAD) ray-tracing computer program. In addition, we designed, fabricated, and tested an optical system using a computer-generated hologram and a computer-originated holographic lens.

ERIM

May 1980

COMPUTER GENERATED HOLOGRAPHIC OPTICS

Environmental Research Institute of Michigan
P.O. Box 8618
Ann Arbor, Michigan 48107

128600-12-F

FINAL REPORT

PERIOD COVERED: 1 April 1977 to 31 March 1980
CONTRACT NUMBER: DAAG29-77-C-0017
ARO PROJECT NUMBER: P-14582-EL
AUTHOR & PRINCIPAL INVESTIGATOR: James R. Fienup

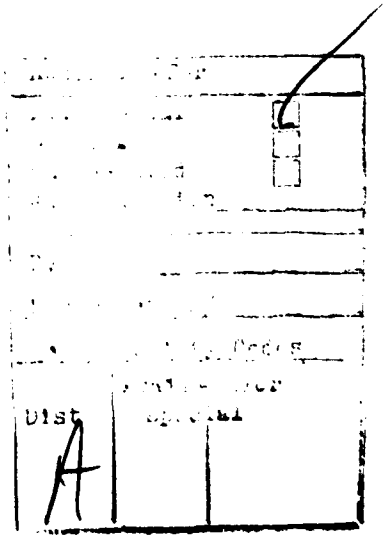

COMPUTER GENERATED HOLOGRAPHIC OPTICS

STATEMENT OF THE PROBLEM STUDIED

The goal of this research was to theoretically and experimentally investigate the use of computer-generated holograms in the design and fabrication of holographic optical elements (holographic lenses or diffraction optics). Conventional design of holographic lenses had previously been limited to spherical recording beams, and more recently to recording beams formed by conventional optical systems. The utilization of computer-generated holograms in the recording beams allows a completely arbitrary specification of the recording wavefronts in the hologram plane, making possible a hologram lens of higher performance (lower aberrations) than previously possible. We refer to an interferometrically recorded hologram lens having a computer-generated hologram in a recording beam as a computer-originated holographic lens. We studied the basic limitations of computer-generated holograms, and integrated the analysis of computer-generated holograms and computer-originated holographic optical elements into ERIM's holographic optical analysis and design (HOAD) ray-tracing computer program. In addition, we designed, fabricated, and tested an optical system using a computer-generated hologram and a computer-originated holographic lens.

SUMMARY OF RESULTS

Several different types of computer-generated holograms were studied and evaluated for this application. Important considerations are the diffraction efficiency, the type of optical recording device required (binary vs grey-level), the spatial efficiency with which the recorder is utilized, the type of recording material required (absorbing vs phase shifting), the recording material properties, and the intrinsic errors (e.g. spurious diffracted terms) arising from the computer-generated hologram. For achieving high performance holographic lenses, the most important consideration of those listed above is the minimization of intrinsic errors and spurious

terms. Given the availability of a grey-level recording device, we concluded that the simple carrier method is the computer-generated hologram best suited for this application. It consists of a carrier-frequency encoding of the phase plus a bias, resulting in a real, nonnegative transmittance of the form: bias + amplitude · cos [ωx + phase (x, y)].

Computer-generated holograms are not very useful as optical elements by themselves since they have low diffraction efficiency, low numerical aperture (i.e. low space-bandwidth product), and intrinsic spurious orders of diffraction. However, all of these deficiencies can be avoided by interferometrically recording a holographic optical element on a volume-phase material of high diffraction efficiency, such as dichromated gelatin, using a computer-generated hologram in one of the recording beams. Referred to as a computer-originated holographic optical element (COHOE), it can have a high numerical aperture if one or both of its recording beams is produced by a conventional optical system in conjunction with the computer-generated hologram. This is described further in Appendix A. Appendix A also describes the implementation of an analysis capability for computer-generated holograms and COHOEs within the HOAD program. The design, analysis, fabrication and testing of an optical system employing a computer-originated holographic lens, using a computer-generated hologram in one of its recording beams, is also described. By this method we arrived at a holographic lens having far lower aberrations than a holographic lens made with conventional spherical recording beams. When used as a Fouier transform element, this aspheric holographic lens achieves close to an order of magnitude improvement in two-dimensional space-bandwidth product capacity as compared with a conventionally recorded holographic Fourier transform element. This new technology, which we have demonstrated to be feasible, is expected to generally provide better performance with fewer optical elements than what was previously obtainable.

In the course of examining the imaging of computer-generated holograms from one plane to another, we studied the imaging of wavefronts. In contrast to imaging an intensity distribution, the imaging of a wavefront by an optical system is complicated by the fact that the phase of the wavefront in addition to its intensity must be handled properly. Except for special cases, there is

an additional quadratic phase factor present. Analysis was performed to compute the wavefront image position, magnification and additional quadratic phase factor for general one-lens and two-lens imaging systems. It was found that by using two lenses of fixed focal length it is possible to obtain both a given magnification and a given quadratic phase factor, within certain limits. The range of obtainable magnifications and quadratic phase factors, it was also found, can be expanded by using three-lens or four-lens imaging systems.

Application of computer-originated holographic optics to variable phase compensators was also analyzed. It was determined that three holographic phase plates can be used to produce variable (adaptive) amounts of one-dimensional cubic and quartic phase correction by the translation of the second and third phase plates with respect to the first phase plate. Used in conjunction with a conventional optical processor for synthetic aperture radar imaging, these phase plates would allow for the compensation of several wavelengths of phase error in the radar signal history. This task is currently very difficult to perform in a dynamic manner using conventional optics.

Computer experiments and analysis were also performed on a special holographic diffuser that would cause a minimum of speckle in a reconstructed image. The holographic diffuser would be made from a computer-generated hologram. It is briefly described in Appendix B.

PUBLICATIONS

J.R. Fienup, "Checkerboard Real-Imaginary Phase Code," J. Opt. Soc. Am. 68, 1444 (October, 1978).

R.C. Fairchild and J.R. Fienup, "Holographic Optical Elements Recorded with Arbitrary Wavefronts," J. Opt. Soc. Am. 69, 1429 (October 1979).

R.C. Fairchild and J.R. Fienup, "Computer-Originated Hologram Lenses," Proceedings of the SPIE 215-01, Recent Advances in Holography (February, 1980).

PARTICIPATING SCIENTIFIC PERSONNEL

Personnel responsible for the research performed under this contract were Dr. J.R. Fienup and R.C. Fairchild. Other participating scientific personnel were W.S. Colburn and Dr. W. Holsztynski.

The research performed by R.C. Fairchild will be included in his PhD dissertation at the University of Michigan.

ERIM

Appendix A

Computer-Originated Hologram Lenses

R.C. Fairchild and J.R. Fienup

Presented at the Symposium of the
Society of Photo-Optical Instrumentation Engineers
in Los Angeles, California, February 4, 1980
and Published in the Proceedings of the SPIE 215-01
Recent Advances in Holography

Computer-Originated Hologram Lenses

R.C. Fairchild and J.R. Fienup

Radar and Optics Division
Environmental Research Institute of Michigan
P.O. Box 8618, Ann Arbor, Michigan 48107

Abstract

The capability of analyzing hologram lenses recorded with arbitrary wavefronts has been added to a holographic raytracing design program. The recording wavefronts are defined by analytical phase functions, for example, a two-dimensional polynominal expansion. The coefficients of the functional representations of the recording wavefronts are used as parameters to optimize the performance of an optical system containing the hologram lens. The optimum recording wavefronts are then produced with the help of computer-generated holograms. Several useful arbitrary wavefront phase functions are discussed. Design predictions and experimental results will be shown for a holographic Fourier transform lens recorded with the aid of a computer-generated hologram.

Introduction

The past several years has seen an increased use of refractive optical elements having aspheric surfaces. The generalization of lens surface profiles has produced better system performance with fewer elements in many applications. It is reasonable to suppose, therefore, that holographic optical elements (HOEs) would also benefit from the use of generalized recording wavefronts (Figure 1). The design of diffractive optical systems has until recently been restricted to the use of HOEs recorded with plane and/or spherical wavefronts (Figure 2). These wavefronts are the ones most readily generated in the laboratory using standard refractive optical components. The generation of truely arbitrary recording wavefronts using refractive optics, on the other hand, is difficult at best. A more feasible approach is the use of a computer-generated hologram (CGH) to optically generate the desired arbitrary aspheric recording wavefront[1]. The increasing availability and performance of devices for recording CGHs makes this an attractive approach.

This paper describes the implementation of an aspheric HOE design capability within an existing holographic raytrace program. Consideration is given to methods for defining arbitrary recording wavefronts on curved as well as flat substrates. In addition, techniques for defining CGHs to generate the desired arbitrary recording wavefronts are presented. Finally, the design of a simple aspheric HOE to be used as a Fourier transform (F.T.) lens is described and experimentally evaluated.

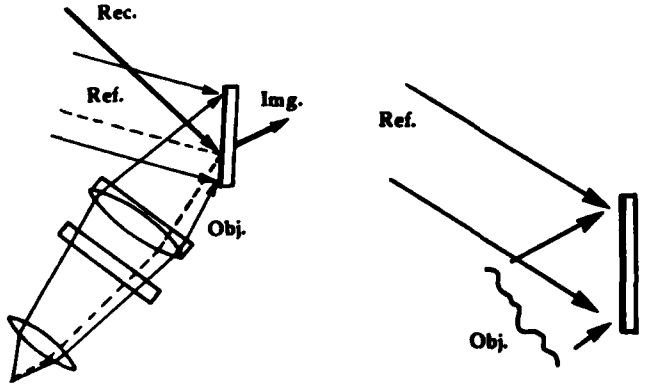

Figure 1. Aspheric HOEs are recorded with an object wavefront (a) derived from an auxiliary optical system or (b) defined analytically.

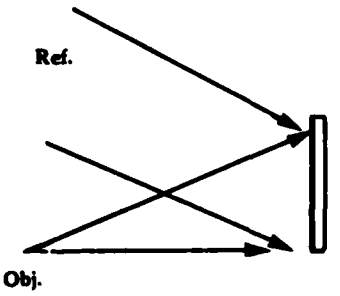

Figure 2. Conventional (spherical) HOEs are recorded with spherical and/or plane wavefronts.

Raytracing through HOEs

A short discussion of the raytrace grating equations is appropriate at this point. We assume that a HOE is recorded with an object beam (Obj) and a reference beam (Ref) as depicted in Figure 1a. In this case, the object beam is shown to be derived from an auxiliary optical system. During the raytrace through the optical system under consideration (the "primary" system), a reconstruction ray (Rec) impinges upon the hologram, is diffracted by the hologram and results in an image ray (Img). The phase and direction of propagation of the image ray is determined by the phases and directions of the reconstruction, reference and object rays at the reconstruction ray intercept. A simplified form of the grating equations which determine the image ray is as follows.

$$\phi_I = \phi_C \pm \frac{\lambda_C}{\lambda_0}(\phi_0 - \phi_R) \tag{1}$$

$$l_I = l_C \pm \frac{\lambda_C}{\lambda_0}(l_0 - l_R) \tag{2}$$

$$m_I = m_C \pm \frac{\lambda_C}{\lambda_0}(m_0 - m_R) \tag{3}$$

$$n_I = \pm\sqrt{1 - l_I^2 - m_I^2} \tag{4}$$

where ϕ is the ray phase, λ_C is the readout wavelength, λ_0 is the recording wavelength, l, m and n are the x, y and z direction cosines, respectively; and subscripts I, C, O and R refer to the image, reconstruction, object and reference rays, respectively. The sign choice in Equations 1-3 is used to select either the principal diffracted wavefront (+) or the conjugate wavefront (-). The sign choice in Equation 4 is used to select the z-direction of propagation of the wavefront.

In the typical raytrace problem, the phase and direction cosines of the reconstruction ray is known, either as input to the system or as the result of a raytrace through a preceding element. The phases and direction cosines of the object and reference rays, however, must be determined based upon the reconstruction ray intercept. For the case of a spherical HOE in which the object and reference wavefronts are restricted to being either plane or spherical wavefronts, the task is a simple one. The phase and direction cosines of a ray passing through any point illuminated by the wavefront are easily calculated based upon the direction of the plane wavefront or the location of the spherical point source. The case of an aspheric HOE, however, may present a more difficult task depending upon the way in which the arbitrary recording wavefront is defined.

The two principle ways of detining an arbitrary wavefront are (1) by the specification of an auxiliary optical system that is used to generate the wavefront (Figure 1a) or (2) by an analytical description of a wavefront defined on a surface (Figure 1b). In this paper we discuss both ways of describing arbitrary recording wavefronts, with emphasis on the analytical description on a surface.

Arbitrary recording wavefronts derived from auxiliary optical systems

The task of determining the phase and direction cosines of a recording wavefront derived from an auxiliary optical system at a given reconstruction ray intercept is indeed a difficult one. There are two basic approaches to solving this problem. The first approach is to trace rays through the auxiliary system in an iterative fashion until the ray which passes through the reconstruction ray intercept is found. The second approach is to trace a grid of rays through the auxiliary system to the HOE, and then during the raytracing of the primary system to perform an interpolation on the grid of rays to obtain the phases and direction cosines at the reconstruction ray intercepts. A two-dimensional interpolation is required which preferably takes into account the known direction cosine samples as well as the phase samples. The interpolation is further complicated by the fact that a regularly spaced grid at the input to the auxiliary optical system will be distorted into an irregular grid at the HOE.

Each of the above approaches has its own advantages and disadvantages. The iterative approach requires that several raytraces through the auxiliary system be performed for each ray traced through the primary system. In general the number of iterative raytraces through the auxiliary system for each primary system raytrace will be small since the arbitrary recording wavefronts of interest for HOEs are well behaved. The interpolation approach, on the other hand, requires that a relatively large number of rays (typically 25 to several hundred) be traced through the auxiliary system once. Thereafter, any number

of rays may be traced through the primary system and only interpolation will be required to determine the phase and direction cosines of the arbitrary recording wavefront at each reconstruction ray intercept. If the auxiliary system contains an optimization variable, however, the grid of rays will need to be retraced each time the variable changes value. The tradeoffs between the two approaches are complex and depend in large part on the relative complexities of the primary and auxiliary systems.

The interpolation approach has been implemented within the Holographic Optics Analysis and Design (HOAD)[2] program at ERIM and has been discussed in detail elsewhere.[3] The remainder of this paper will concentrate on the class of aspheric HOEs for which the arbitrary recording wavefronts are defined analytically at the recording surface.

Analytical arbitrary wavefronts for aspheric HOE design

We have recently added to the HOAD raytrace program at ERIM the capability of analyzing aspheric HOEs recorded with analytically defined wavefronts. The analysis is currently limited to wavefronts which are pure phase functions, i.e., the wavefront amplitude is assumed uniform over the extent of the wavefront. The phase function is assumed to be defined on the surface of the recording medium. The surface (or substrate) can be curved as well as flat. A variety of general analytical phase functions have been supplied for the designer's use including the following.

. Sum of monomials (power series)

$$\phi(x, y) = \sum_{i=0}^{9} \sum_{j=0}^{9} C_{ij}\, x^i y^j \tag{5}$$

. Sum of Legendre polynomials (orthogonal polynomials)

$$\phi(x, y) = \sum_{i=0}^{9} \sum_{j=0}^{9} C_{ij} L_i(x) L_j(y) \tag{6}$$

. Spherical wavefront + sum of monomials

. Spherical wavefront + sum of polynomials

The C_{ij} in Equations (5) and (6) represent the coefficient values of the respective polynomials. Up to 100 coefficients may be specified for each phase function and all may be used as optimization parameters. The maximum of ninth order in x and y was made to limit the amount of computer memory required to store the coefficients of each arbitrary wavefront. In addition to using the preprogrammed phase functions described above, the designer may himself define an explicit phase function utilizing up to 100 optimization parameters. New phase functions are continually being added to the library of available functions in this manner.

There are, of course, limitations upon how quickly any phase function may vary. Specifically, in order to avoid evanescent waves, the following relation must be satisfied,

$$\sqrt{\left(\frac{\partial \phi}{\partial x}\right)^2 + \left(\frac{\partial \phi}{\partial y}\right)^2} \leq \frac{2\pi}{\lambda} \tag{7}$$

where λ is the recording wavelength. Violation of this constraint results in a ray failure during the raytrace.

Flat substrate

Raytracing through a flat aspheric HOE recorded with an analytically defined arbitrary wavefront is a straightforward procedure. The direction cosines of the analytical wavefront at the reconstruction ray intercept, (x_0, y_0), are readily computed from the partial derivatives of the phase function as follows.

$$\phi = \phi(x, y)\big|_{x_0, y_0} \tag{8}$$

$$l_0 = \frac{\lambda}{2\pi} \frac{\partial \phi}{\partial x}\bigg|_{x_0, y_0} \tag{9}$$

$$m_0 = \frac{\lambda}{2\pi} \left.\frac{\partial \phi}{dy}\right|_{x_0, y_0} \tag{10}$$

$$n_0 = \pm\sqrt{1 - l_0^2 - m_0^2} \tag{11}$$

The sign of the z direction cosine given in Equation (11) is chosen to provide the desired direction of propagation. Then, using the grating Equations (1) to (4), the phase and direction cosines of the image ray are computed.

Curved substrate

The use of an analytically defined wavefront to record an aspheric HOE on a curved substrate is somewhat more complex than the flat substrate case. One method of specifying the wavefront would be to define a phase function on the curved surface, in which case the computation of the direction cosines would depend upon the surface function in addition to the phase funtion (Figure 3a). An alternative approach would be to define the phase function on a plane separated from the curved substrate. This latter case is similar to that of defining a wavefront by an auxiliary system in that, in order to find the ray phase and direction cosines at a given intercept, it is necessary to either perform an iterative raytrace (Figure 3b) or trace a grid of rays and use iterpolation. In this case the procedure is simplified by the fact that the raytrace is between two surfaces with no intervening optics. It is particularly simple if the plane is chosen to be a tangent plane of the curved surface.

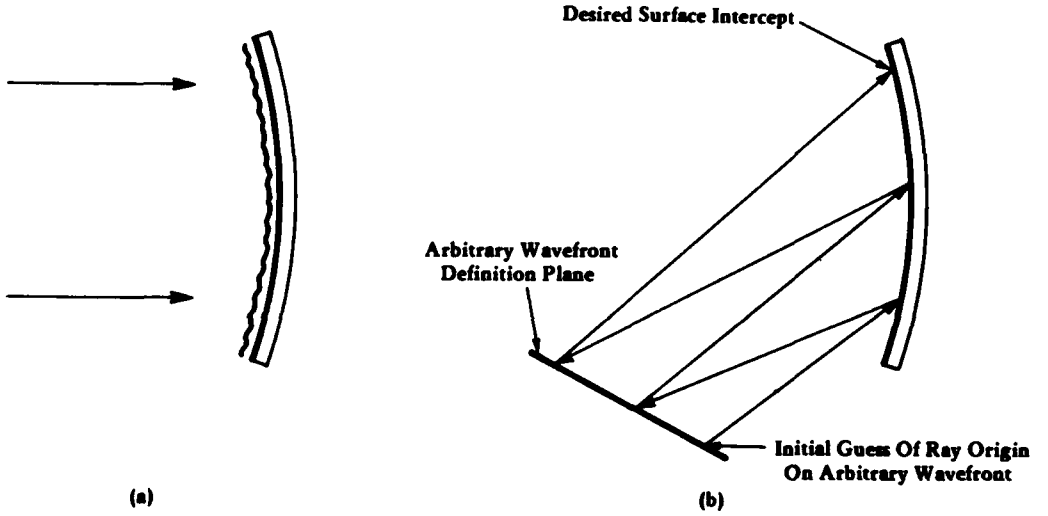

Figure 3. A curved aspheric HOE recorded with an analytically defined wavefront can have that wavefront (a) defined on the curved surface or (b) defined on a plane separated from the surface.

We have chosen to implement the first method in which the phase function is defined on the curved surface. The analysis proceeds as follows. Let the phase of a wavefront throughout a certain volume be $\phi(x, y, z)$. Assuming that the wavefront forms a normal congruence (i.e., rays do not cross one another and the phase and direction cosines are uniquely defined at every point), the wavevector is given by

$$\vec{k} = k_x\hat{x} + k_y\hat{y} + k_z\hat{z} = \nabla\hat{\phi}(x, y, z) \tag{12}$$

where $\hat{x}$, $\hat{y}$, and $\hat{z}$ are the cartesian unit vectors. The direction cosines are given by

$$l = k_x/k = \frac{1}{k}\frac{\partial\hat{\phi}}{\partial x} \tag{13}$$

$$m = k_y/k = \frac{1}{k}\frac{\partial\hat{\phi}}{\partial y} \tag{14}$$

and

$$n = k_z/k = \frac{1}{k}\frac{\partial\hat{\phi}}{\partial z} \tag{15}$$

where

$$k = |\bar{k}| = \frac{2\pi}{\lambda} = \frac{2\pi n_i}{\lambda_0} \tag{16}$$

where λ_0 is the wavelength of light in a vacuum and n_i is the index of refraction. The phase evaluated at a surface

$$z = z(x, y) \tag{17}$$

is given by

$$\phi(x, y) = \hat{\phi}[x, y, z(x, y)] \tag{18}$$

which we refer to as the surface phase function. Having defined the surface phase function $\phi(x, y)$ by an analytical expression, the problem is to recover the direction cosines which are proportional to the partial derivatives of $\hat{\phi}(x, y, z)$, which are different from the partial derivatives of $\phi(x, y)$. By the chain rule of partial derivatives, we have the two equations

$$\frac{\partial\phi}{\partial x} = \phi_x = \frac{\partial\hat{\phi}}{\partial x} + \frac{\partial\hat{\phi}}{\partial z}\frac{\partial z}{\partial x} \tag{19}$$

and

$$\frac{\partial\phi}{\partial y} = \phi_y = \frac{\partial\hat{\phi}}{\partial y} + \frac{\partial\hat{\phi}}{\partial z}\frac{\partial z}{\partial x} \tag{20}$$

and, in addition, taking the magnitude squared of Equation (12) we have the condition

$$k^2 = \left(\frac{\partial\hat{\phi}}{\partial x}\right)^2 + \left(\frac{\partial\hat{\phi}}{\partial y}\right)^2 + \left(\frac{\partial\hat{\phi}}{\partial z}\right)^2 \tag{21}$$

Solving the three simultaneous Equations (19), (20) and (21) for the three unknowns, we find that

$$\frac{\partial\hat{\phi}}{\partial z} = \hat{\phi}_z = \frac{(\phi_x z_x + \phi_y z_y) \pm \sqrt{(\phi_x z_x + \phi_y z_y)^2 + \left(1 + z_x^2 + z_y^2\right)\left(k^2 - \phi_x^2 - \phi_y^2\right)}}{\left(1 + z_x^2 + z_y^2\right)} \tag{22}$$

$$\frac{\partial\hat{\phi}}{\partial x} = \phi_x - \hat{\phi}_z z_x \tag{23}$$

$$\frac{\partial\hat{\phi}}{\partial y} = \phi_y - \hat{\phi}_z z_y \tag{24}$$

where $z_x = \partial z(x, y)/\partial x$ and $z_y = \partial z(x, y)/\partial y$. The computation of the phase and direction cosines from the surface phase function using Equations 22 to 24 is very straightforward in contrast with the method of defining the phase on a plane separated from the curved surface. Unlike that method, however, the definition of the phase on the curved surface causes a strong coupling between the wavefront $\hat{\phi}(x, y, z)$ and the shape of the surface $z(x, y)$.

Recording techniques for aspheric HOEs

Once a recording wavefront is established by the designer, it becomes necessary to produce that wavefront in the laboratory. For the case of a recording wavefront defined by an auxiliary system as depicted in Figure 1a, the procedure is straightforward: an optical system corresponding to the auxiliary system must be assembled. For the case of an analytically defined arbitrary wavefront, on the other hand, the design itself does not suggest a method of arriving at the desired wavefront.

One method would be to record the desired aspheric HOE as a CGH. Several inherent limitations of CGHs, however, severely limit the direct use of a CGH as a HOE. First and foremost, optical recording devices used to generate CGHs are limited in spatial resolution and space-bandwidth product, restricting the angles of diffraction and numerical apertures of the CGH. In addition, unwanted orders of diffraction and other spurious terms are usually present in a CGH. These further restrict the usable diffraction angles and field-of-view if interference with these undesired terms is to be avoided. Another limi-

tation is the low value of the maximum diffraction efficiencies for most types of CGHs. The maximum diffraction efficiency for a thin amplitude hologram is 6.25%, for a binary amplitude hologram 10.13%, and for a thin phase hologram 33.9%.[5] Types of CGHs that have diffraction efficiencies approaching 100%, such as the kinoform[6] and the ROACH,[7] are more difficult to generate accurately.

All of the above limitations can be circumvented, however, through the use of a HOE recorded with a CGH in one of the recording beams, instead of using the CGH itself as the optical element. By using a volume phase material, such as dichromated gelatin[8] for the HOE, diffraction efficiencies approaching 100% are achieved and spurious orders of diffraction are minimized. By combining appropriate optics with the CGH in the recording beam, the resolution and the space-bandwidth product required of the CGH can be greatly reduced.[9] In addition, spatial filtering can be performed in order to remove spurious terms inherent in the CGH.

The first step is to design a recording system that reduces the space-bandwidth product and resolution requirements of the CGH. It is assumed that the recording wavefront of the HOE has already been specified as an analytical arbitrary wavefront. Then the raytrace program is used to back propagate the desired recording wavefront through a recording optical system to a CGH plane (Figure 4a). The recording optical system will ordinarily be designed to remove tilt, focus, and other low-order phase terms which tend to be large in magnitude. A secondary purpose of the recording optical system is to provide a frequency plane in which a spatial filter may be used to remove the undesired diffracted orders of the CGH. Once the recording optical system is designed to produce a wavefront with acceptably low space-bandwidth product at the CGH plane, a grid of rays is back propagated from the hologram to the CGH to provide samples of the phase fucntion that is to be recorded as a CGH. A frequency offset must be added during the CGH recording process to insure that the zero-order and second-order diffracted terms do not overlap the desired first order diffracted term in the frequency plane. The amplitude transmittance of the CGH then has the form

$$t_a = b + m \cos [\omega x + \phi(x, y)] \qquad (25)$$

where $b = 0.5$ is a bias, $m \leq 0.5$ is the modulation, and ωx is the carrier frequency offset.

For this Burch-type[10] CGH (simple carrier frequency), an offset slightly larger than one half of the double-sided bandwidth of the wavefront is required. This is less than that generally required by an optically generated hologram because the Burch type CGH does not record the object autocorrelation term which has twice the bandwidth of the object wavefront. However, in order to avoid spurious terms that would arise in the event of a nonlinear amplitude transmittance, it may be necessary to use a carrier frequency that is 1.5 times the double-sided bandwidth of the wavefront.[5]

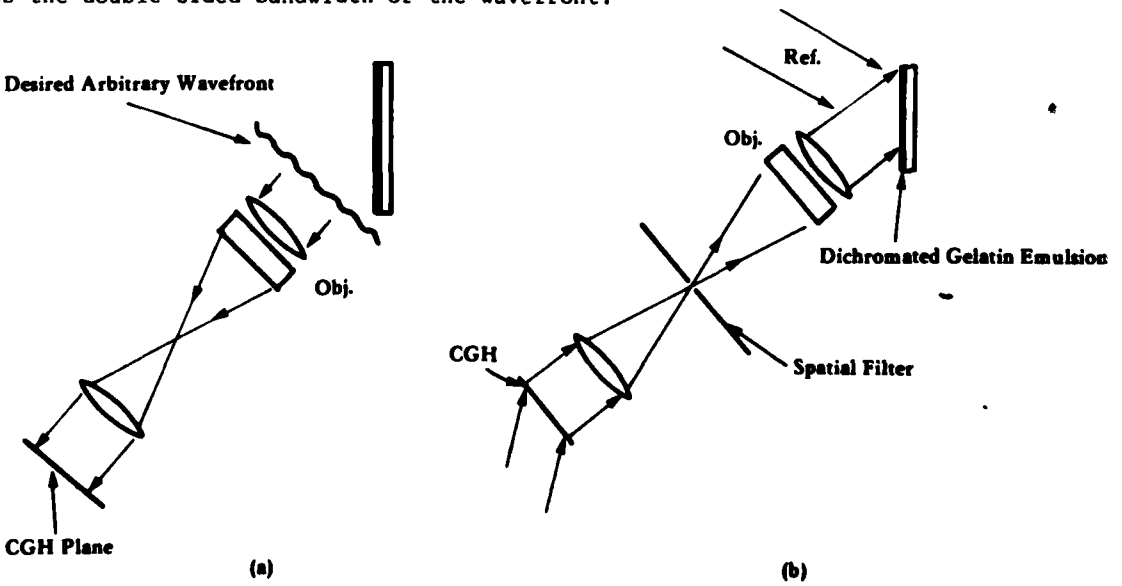

Figure 4. COHOE recording process. (a) After the desired arbitrary recording wavefront is defined it is backwards raytraced through an auxiliary recording system to a CGH definition plane. (b) The COHOE is recorded on a high efficiency medium using the CGH and optical system as defined in (a).

Finally, the CGH is fabricated and assembled with the recording system (Figure 4b) to provide the desired recording wavefront at the HOE. The HOE which is recorded in this manner we call a computer-originated HOE (COHOE). In the following sections we discuss an example of the design of an aspheric HOE and its implementation as a COHOE.

An aspheric HOE design example

To demonstrate the use of an analytical arbitrary recording wavefront we designed a Fourier transform HOE which could be used in a coherent optical processor (Figure 5). A transparency at the input plane is illuminated by a coherent plane wavefront. The input transparency produces an angular spectrum of plane wavefronts (one for each spatial frequency component of the input) which propagate to the Fourier transform HOE. The HOE causes them to be focused to points in the output plane. The higher spatial frequencies in the input transparency diffract the illuminating wavefront at proportionately higher angles and come to focus farther from the center of the output plane.

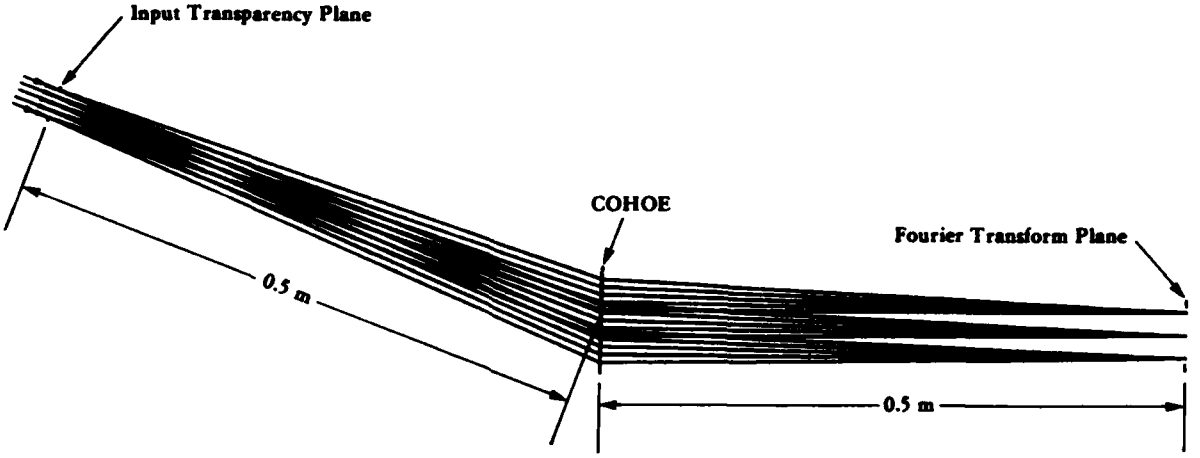

Figure 5. Fourier transform HOE readout geometry. Three bundles of five parallel input rays each are shown propagating from the input plane to the Fourier transform plane. Each of the three ray bundles represents a different plane-wave spatial frequency component which comes to focus at a point in the transform plane.

In a previous design effort to produce such a Fourier transform HOE[11] using conventional spherical wavefronts, it was determined that optimum performance over a range of input spatial frequencies was achieved with a recording geometry as shown in Figure 6. The point source for the object recording wavefront should be on an axis normal to the HOE at a point corresponding to the center of the output plane.

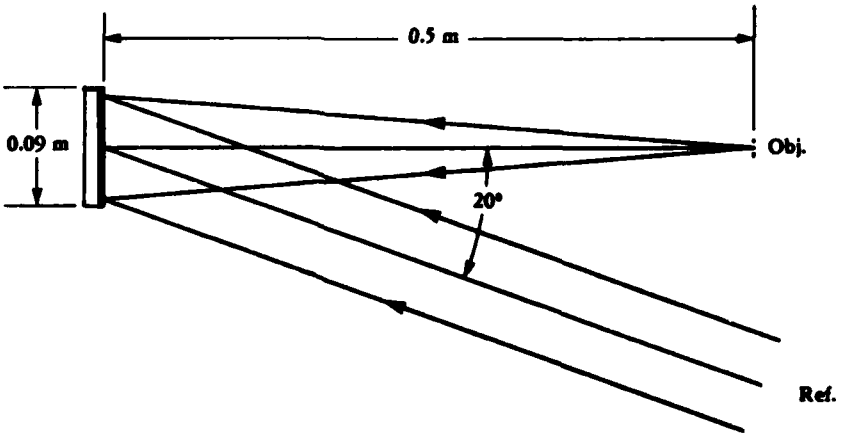

Figure 6. The optimized recording geometry for a conventional Fourier transform HOE using plane and spherical wavefronts.

Using this previous design as a starting point, we further optimized the HOE, allowing the tilted plane reference wavefront to be perturbed by the following polynomial phase function.

$$\phi(x, y) = 2\pi\left[C_{20}x^2 + C_{40}x^4 + C_{60}x^6 + C_{80}x^8 + C_{02}y^2 + C_{04}y^4 + C_{06}y^6 + C_{08}y^8 + C_{22}x^2y^2 + C_{44}x^4y^4\right] \quad (26)$$

All ten of the C_{ij} coefficients were allowed to vary during a damped least-squares optimization. Twenty-one rays forming a pair of orthogonal fans on a 25 mm diameter input aperture (Figure 7a) were raytraced to the Fourier transform plane for each system solution in the optimization. The focal length of the HOE was designed to be 0.5 meters and the recording and readout wavelengths were both 514.5 nm. The merit function consisted of the sum of squares of the RMS spot size at the Fourier transform plane for ten illumination angles: $\alpha = -2.4^\circ, -1.2^\circ, 0^\circ, 1.2^\circ, 2.4^\circ$ (in the x-z plane) and $\beta = -2.4^\circ, -1.2^\circ, 0^\circ, 1.2^\circ, 2.4^\circ$ (in the y-z plane). The resultant optimized coefficients are given in Table 1. The coefficients of Table 1 are normalized to have units of wavelengths (λ) and the x and y coordinates are scaled such that $-1 \leq x, y \leq 1$ over the hologram recording area (i.e., x and y are unitless). A perspective plot of the optimized phase correction is shown in Figure 8. Aberration plots which compare the primary aberrations of the starting design (conventional spherical HOE) and the optimized aspheric HOE as a function of field angle α(x-z plane) are depicted in Figure 9.

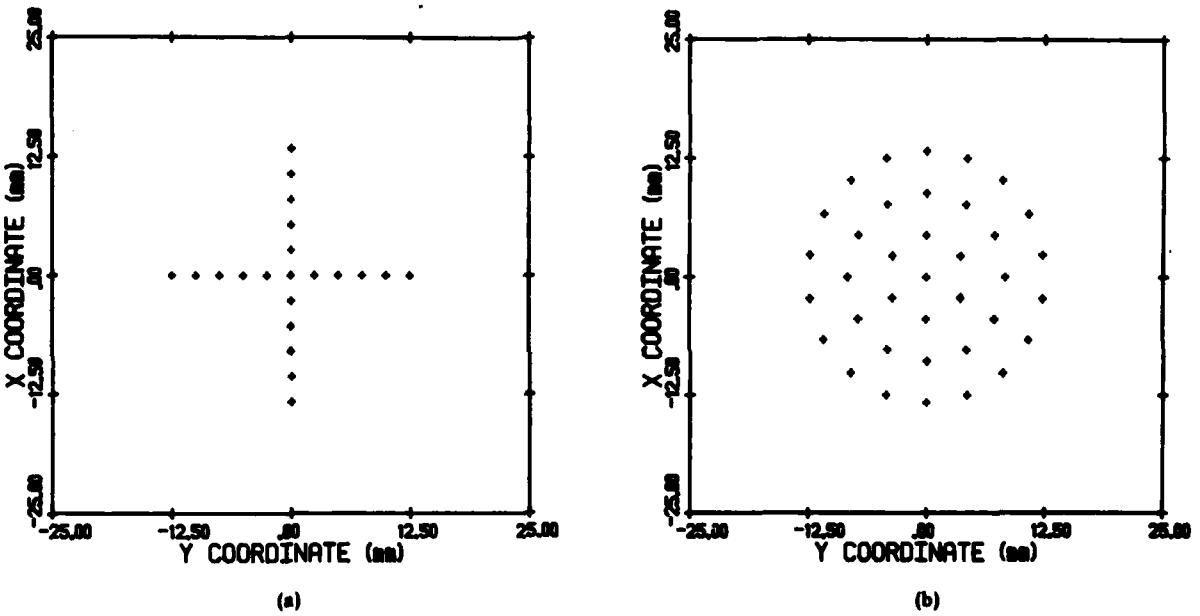

Figure 7. Raytrace input ray distributions used for (a) aberration calculations (orthogonal fans) and (b) spot diagrams (hexapolar array).

Table 1. Optimized Coefficients for an Aspheric Fourier Transform HOE

$C_{20} = .714$	$C_{02} = 1.569$	$C_{22} = 1.908$
$C_{40} = 4.092$	$C_{04} = 2.194$	$C_{44} = 64.619$
$C_{60} = 3.150$	$C_{06} = 4.036$	
$C_{80} = -.964$	$C_{08} = .502$	

The conventional HOE design exhibits large amounts of misfocus (field curvature) and coma and essentially no spherical aberration. The aspheric HOE design has significantly reduced the misfocus and coma at the expense of introducing some spherical aberration. The total RMS aberration shows a total reduction from a peak of 0.297 λ for the conventional HOE to a peak of 0.038 λ for the aspheric HOE design. Similarly the RMS spot size was reduced from 40.17 μm peak for the conventional HOE to 6.56 μm peak for the aspheric HOE design. No attempt was made to reduce distortion, although this should be possible with the proper merit function. The next section will describe an experimental verification of the design results presented in this section.

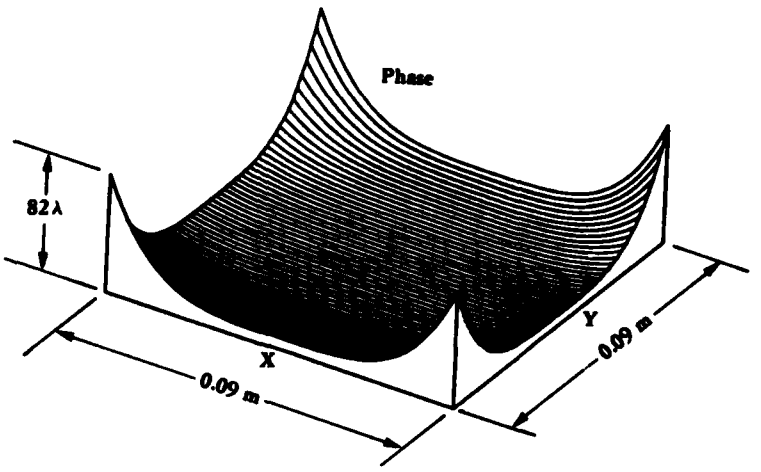

Figure 8. Three-dimensional plot of the optimized aspheric phase correction to the reference recording wavefront of a Fourier transform HOE (as defined by Table 1).

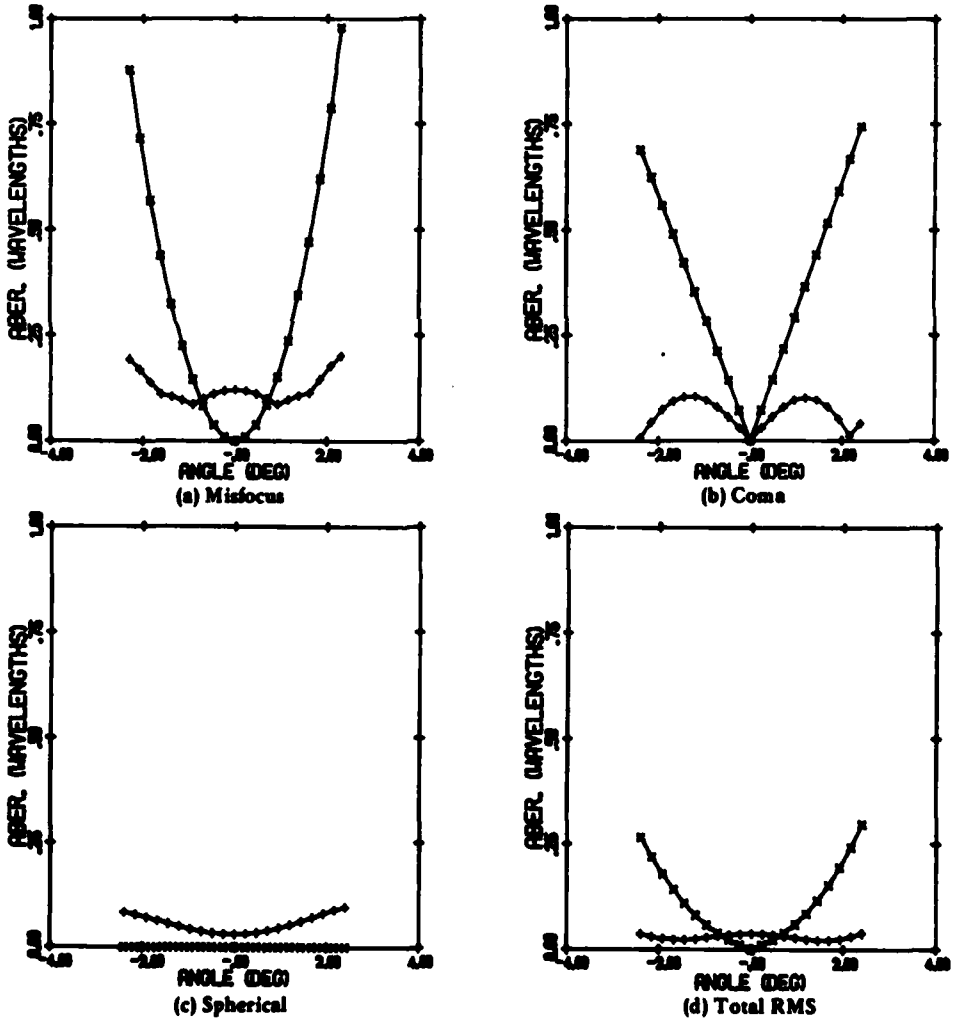

Figure 9. Aberration plots comparing the performance of a conventional Fourier transform HOE (x's) and an aspheric Fourier transform HOE (+'s).

Recording and evaluation of an aspheric HOE

The aspheric Fourier transform HOE design described in the last section was recorded as a COHOE using the optical system diagrammed in Figure 10. The diffracted wavefront from the CGH is reimaged at the COHOE recording plane by a one-to-one telescope. This telescope not only performs imaging from the CGH plane to the COHOE plane, but it also preserves the desired phase relationships (i.e., it does not introduce an extra spherical phase term as would imaging with a single lens). For this case it was assumed that the imaging system adds no extra phase terms, so in the design it was not necessary to simulate the effects of the imaging system. A spatial filter mask is positioned at the frequency plane such that only the desired first-order diffracted wavefront of the CGH is passed to the recording plane. The tilt of the COHOE is such that the desired 20° offset angle is obtained at the recording plane. A slight additional tilt is added to allow for the angle that the first order diffracted term makes with the optical axis as it exits from the telescope. The CGH is similarly tilted so that it and the COHOE are in conjugate image planes. An objective and pinhole assembly provides the required point source object beam.

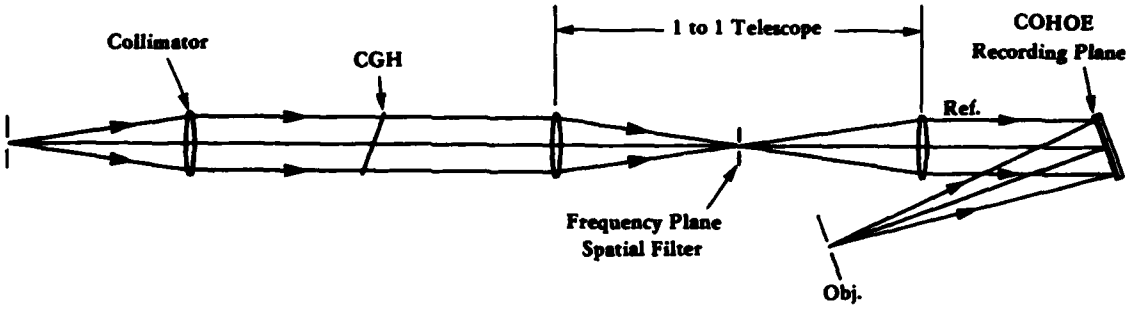

Figure 10. The COHOE recording geometry used to produce a Fourier transform HOE with an aspheric reference wavefront as defined by Table 1.

The optimized arbitrary recording wavefront described by Equation (25) and Table 1 has maximum bandwidths of 0.747 cyc/mm in the x dimension and 0.758 cyc/mm in the y dimension when evaluated over a 90 mm diameter aperture. This wavefront was recorded as a CGH on an Optronics Model 1600 film recorder after a carrier frequency of 3 cyc/mm and a bias were added. The film recorder was operated with a 50 μm square recording spot on a 50 μm sample spacing. The Optronics Model 1600 film recorder is also capable of recording a 25 μm aperture on a 25 μm sample spacing with reduced speed. The Optronics film recorder has a rotating drum with a translating LED and uses Kodak Linagraph Shellburst film #2474. The CGH was contact copied onto a Kodak #649F microflat plate for insertion into the COHOE recording system. The microflat substrate minimized undesired phase errors due to variations in substrate thickness. Similarly, the COHOE was recorded on a Kodak #131-01 microflat plate to insure that phase errors were not introduced during readout. The recording of

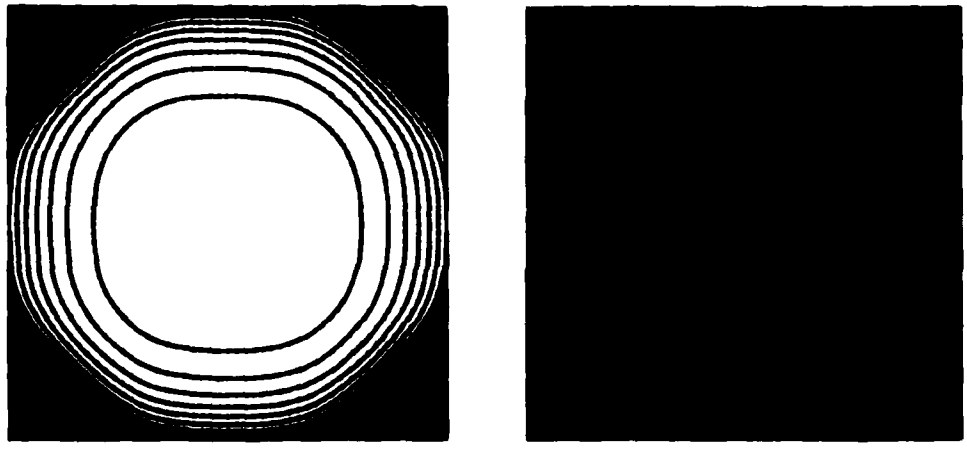

(a) (b)

Figure 11. Interferograms of the aspheric wavefront defined by Table 1 (a) as predicted by a computer raytrace and (b) as optically recorded.

the COHOE utilized 514.5 nm light from an Argon-ion laser. A computer-predicted interferogram of the desired wavefront correction was plotted (Figure 11a) and compared with an optically derived interferogram of the wavefront as recorded by the COHOE (Figure 11b). The agreement was excellent, indicating that no significant phase errors were inadvertently introduced by the recording system.

The performance of the COHOE was evaluated using a rotatable mirror positioned at the input transparency plane (Figure 12). In this manner, a single stationary plane wavefront was made to simulate the wavefront that would be produced by any single spatial frequency at the input transparency plane. A microscope attached to a precision translation device was positioned such that it was focused on the Fourier transform plane of the COHOE.

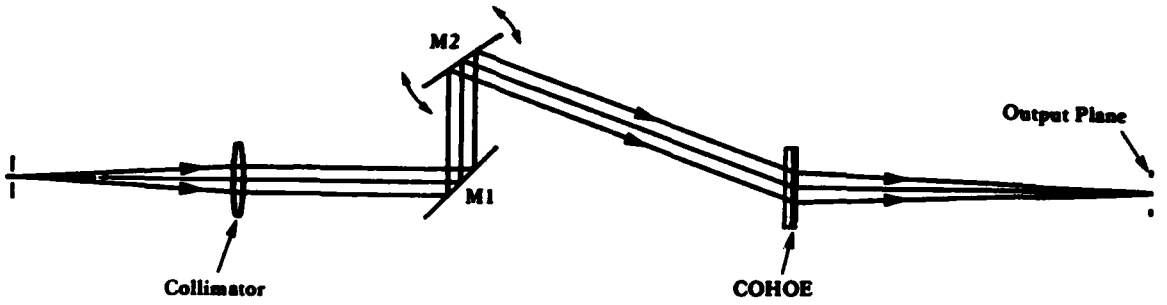

Figure 12. Optical arrangement for evaluating the performance of the aspheric Fourier transform COHOE using a rotatable mirror (M2) at the input transparency plane to simulate any single plane-wave spatial frequency component.

The rotatable mirror was positioned sequentially at the design field angles and the resulting spot sizes in the Fourier transform plane were recorded on film. A comparison of the computer predicted spot sizes of Figure 13 with the corresponding measured spot sizes of Figure 14 indicates excellent agreement. The computer generated spot diagrams were generated by raytracing a hexapolar distribution of rays (Figure 7b) at each of the specified field angles. These spot measurements were made with an input aperture size of 35.6 mm which is somewhat larger than the design size of 25.4 mm. The impulse response of the COHOE recording system has been included in Figure 14 for comparison. The predicted improvement in performance of the COHOE as compared with the conventional (spherical) HOE, particularly at the large field angles, is verified.

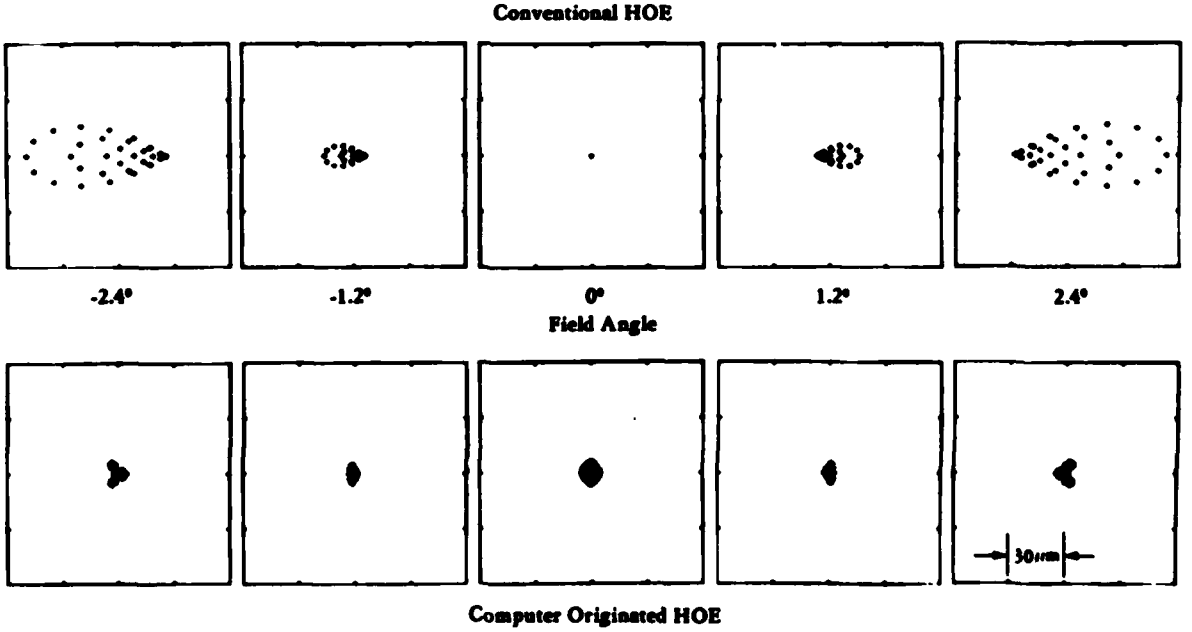

Figure 13. Computer predicted spot sizes of the conventional and computer originated Fourier transform HOEs.

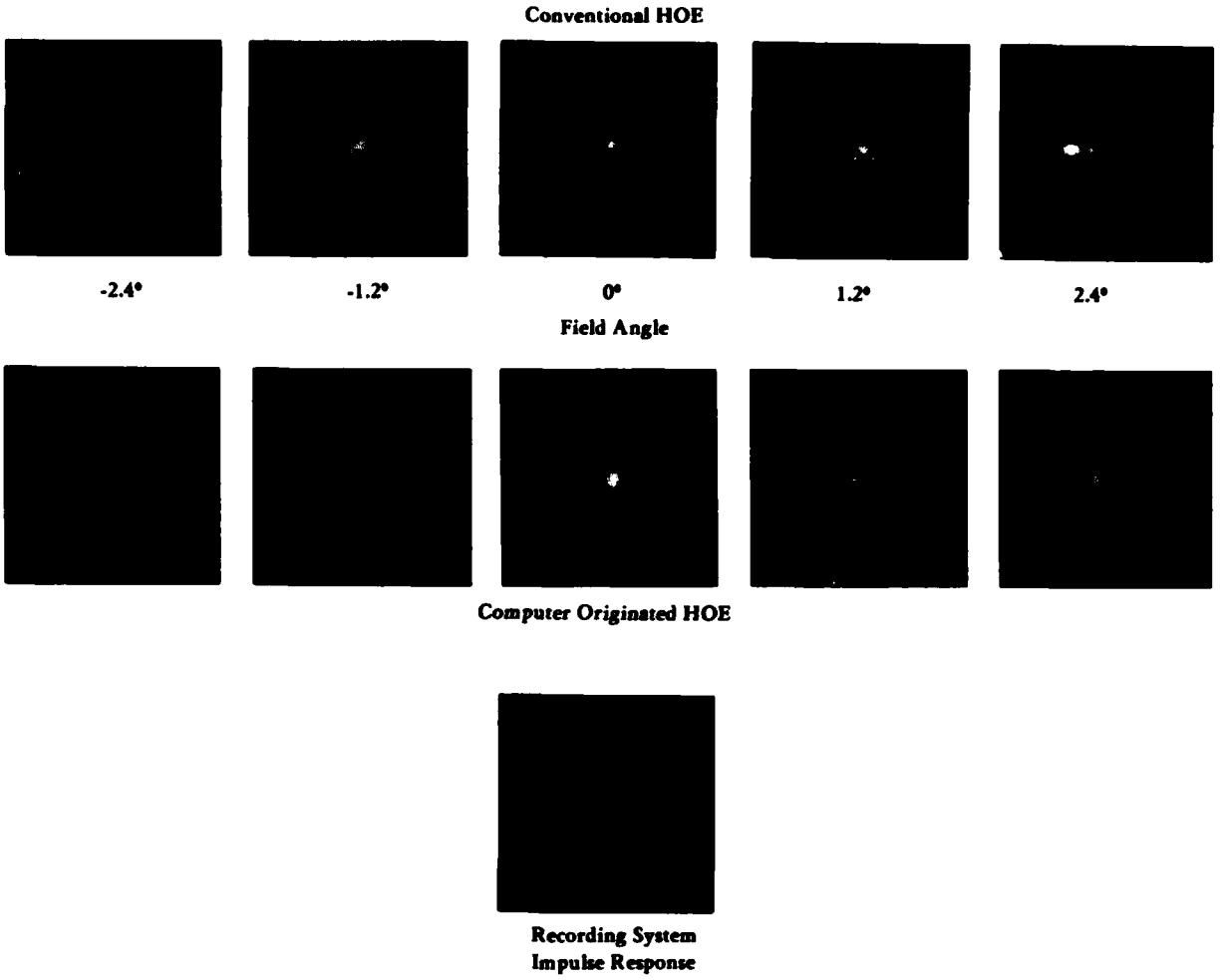

Figure 14. Optically recorded spot sizes of the conventional and computer originated Fourier transform HOEs using the setup shown in Figure 12.

Conclusions

In summary, the work reported in this paper has demonstrated the feasibility of analyzing and implementing aspheric holographic optical elements using analytic descriptions of the recording wavefronts during the design phase and using a CGH in the recording beam during fabrication. The inherent properties of computer-generated holograms which limit their direct use as holographic optical elements are avoided by using the COHOE recording technique. An aspheric Fourier transform HOE was designed which demonstrated a significant improvement in performance when compared to a conventional HOE recorded with spherical wavefronts. It is our opinion that aspheric HOEs will prove to be generally valuable in the design of future high-performance holographic optical systems. In particular we expect that aspheric HOEs will provide better performance with fewer elements and will lessen the burden on the refractive optics in hybrid systems.

Acknowledgements

The authors wish to acknowledge useful discussions with W. Colburn and his numerous contributions to the HOAD raytrace program. This work was supported by the U.S. Army Research Office under contract DAAG29-77-C-0017.

References

1. W.H. Lee, "Computer-Generated Holograms: Techniques and Applications," in E. Wolf, ed., Progress in Optics, Vol 16 (North-Holland 1978).

2. J.N. Latta and R.C. Fairchild, "New Developments in the Design of Holographic Optics," Proc. of the SPIE 39, Applications of Geometrical Optics, 107 (1973); J.N. Latta, "Computer-Based Analysis of Holography Using Ray Tracing," Appl. Opt. 10, 2698 (1971).

3. J.R. Fienup, "Analysis of Holographic Optics for Optical Processors," Interim Scientific Report, AFOSR/NE contract FF44620-76-C-0047, ERIM Report No. 119400-1-T, March, 1977.

4. T.S. Huang, "Digital Holography," Proc. IEEE 59 1335 (1971).

5. R.J. Collier, C.B. Burckhardt and L.H. Lin, Optical Holography, (Academic Press 1971).

6. L.B. Lesem, P.M. Hirsch and J.A. Jordan, Jr., "The Kinoform: A New Wavefront Reconstruction Device," IBM J. Res. Develop. 13, 150 (1969).

7. D.C. Chu, J.R. Fienup and J.W. Goodman, "Multiemulsion On-Axis Computer-Generated Hologram," Appl. Opt. 12, 1386 (1973); D.C. Chu and J.R. Fienup, "Recent Approaches to Computer-Generated Holograms," Opt. Eng. 13, 189 (1974).

8. B.J. Chang and C.D. Leonard, "Dichromated Gelatin for the Fabrication of Holographic Optical Elements," Appl. Opt. 18, 2407 (1979).

9. S. Lowenthal and P. Chavel, "Reduction of the Number of Samples in Computer Holograms for Image Processing," Appl. Opt. 13, 718 (1974).

10. J.J. Burch, "A Computer Algorithm for the Synthesis of Spatial Frequency Filters," Proc. IEEE 55, 599 (1967).

11. J.R. Fienup and C.D. Leonard, "Holographic Optics for a Matched-Filter Optical Processor," Appl. Opt. 18, 631 (1979).

Appendix B

TITLE: Checkerboard Real-Imaginary Phase Code

AUTHOR: J.R. Fienup

ABSTRACT: This phase code (diffuser) for holography causes the spectrum to be leveled well (reduced dynamic range) and results in a minimum of speckle in the image.

SUMMARY:

In digital holography, phase codes (which are analogous to diffusers in interferometric holography) are applied to the object in order to reduce the dynamic range of its Fourier transform, which is encoded in the computer-generated hologram. This makes it easier to faithfully record the hologram and increases its diffraction efficiency. An undesirable artifact arising from most phase codes (particularly the random phase code) is speckle in the reconstructed image. A smoothed, slowly varying phase code results in less speckle in the image but a greater dynamic range in its Fourier transform. The Checkerboard Real-Imaginary Phase (CRIP) code, when combined with an appropriate weighting at the hologram aperture, results in both a greatly reduced dynamic range and greatly reduced speckle. The CRIP code consists of a checkerboard pattern of ± 1 (pure real) and $\pm i$ (pure imaginary), where the signs are chosen quasi-randomly. A physical interpretation of the origin of the speckle will be described, showing why the CRIP code results in greatly reduced speckle. Experimental results will be shown comparing the CRIP code with other phase codes.

Published in:
J. Opt. Soc. Am. 68, p. 1444 (October 1978).